Journal of Applied Electrochemistry **32**: 11–18, 2002.
© 2002 *Kluwer Academic Publishers. Printed in the Netherlands.*

Electrochemical characterization of radiation-grafted ion-exchange membranes based on different matrix polymers

TANJA KALLIO[1]*, MATTS LUNDSTRÖM[1], GÖRAN SUNDHOLM[1], NADIA WALSBY[2] and FRANCISKA SUNDHOLM[2]
[1]*Laboratory of Physical Chemistry and Electrochemistry, Helsinki University of Technology, PB 6100, FIN-02015 HUT, Finland*
[2]*Laboratory of Polymer Chemistry, University of Helsinki, PB 55, FIN-00014 HY, Finland*
*(*author for correspondence)*

Received 1 January 2001; accepted in revised form 22 October 2001

Key words: conductivity, gas permeability, irradiation grafting, membrane, polymer electrolyte fuel cell

Abstract

Seven proton conducting membranes based on different commercial fluoropolymer films were prepared by radiation grafting with styrene followed by sulfonation. These membranes were studied as candidates for fuel cell electrolyte membranes and compared to Nafion® 105 and 117 with respect to conductivity, oxygen and hydrogen permeability, kinetics of the oxygen reduction reaction (ORR) and performance in a fuel cell. The dependence of the conductivity of the membranes on the relative humidity (RH) and temperature was also determined. The conductivity was observed to depend on the membrane thickness and the water uptake. The dependence of the conductivity on the temperature and the RH was the same for all of the experimental membranes. Reactant gas permeabilities appeared to depend only slightly on the matrix material and no major differences in the Tafel slopes and exchange current densities of the ORR were observed. Membranes with high water uptakes appeared to be less durable in the fuel cell than membranes with low water uptakes. Thus to prepare a membrane that is durable under the fuel cell conditions, the water uptake must remain low even at the expense of the conductivity.

1. Introduction

The polymer electrolyte fuel cell (PEFC) is an attractive alternative for future power production due to numerous advantages such as environmental friendliness and high energy density. However, there are still several problems to be solved in order to achieve a useful practical system. Most commonly used membranes, such as the Nafion® series (E.I. Du Pont de Nemours and Company, USA), are based on perfluorosulfonic acid. They have suitable chemical and physical properties for demanding fuel cell conditions but this kind of membrane is expensive because of the fluorochemistry involved in the synthesis. Therefore new alternative membrane materials are being sought [1].

Radiation grafting is a widely known method to prepare proton conducting membranes offering the advantages of low preparation costs, a high degree of control over the process and the possibility to use pre-processed films. Typically membranes are formed by pre-irradiating the matrix films to create reactive sites, followed by grafting with styrene and finally sulfonation of the grafted styrene in order to turn the membranes into an ionically conducting material. Various fluorine-containing polymers have been modified using this method [2–5]. However, comparison of these radiation-grafted membranes is difficult due to differences in the preparation conditions and the degrees of grafting (DOG).

In this study seven different commercial fluoropolymer films were chosen for investigation. In order to determine the influence of the matrix material on the proton conducting membrane properties irradiation-grafted membranes have been prepared under similar conditions resulting in membranes with comparable DOG = 30–40% [6]. The effect of the matrix material on conductivity, reactant gases permeabilities and oxygen reduction reaction (ORR) kinetics was investigated. Also the behavior and durability of the membranes under actual fuel cell conditions were studied.

2. Experimental

2.1. *Membranes*

The following matrix polymers were selected: 15, 40 and 80 μm thick poly(vinylidene fluoride) films (PVDF), two 80 μm poly(vinylidene fluoride-co-hexafluoropropylene) films containing 6 and 15% HFP (PVDF-co-HFP),

Table 1. DOG, IEC, thicknesses (l) and water uptakes (WU) of the experimental membranes

Membrane	Formula of the matrix material	DOG /%	IEC /meq g^{-1}	l (wet) /μm	l (dry) /μm	WU /g g^{-1}	WU /N(H_2O)/O(SO_3)
PVDFa-g-PSSA		36	1.83	130	90	0.73	22
PVDFb-g-PSSA	id	39	1.83	70	55	0.63	19
PVDFc-g-PSSA	id	36	1.64	35	25	0.66	22
PVDF-co-HFP(6%)-g-PSSA	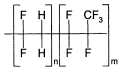	33	1.81	130	90	0.90	28
PVDF-co-HFP(15%)-g-PSSA	id	39	1.94	120	80	1.13	32
FEP-g-PSSA	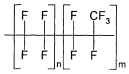	34	1.80	145	80	0.98	30
ETFE-g-PSSA	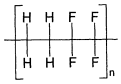	36	1.51	90	55	0.81	30
Nafion 105	–	–	1.00	210	180	0.51	28
Nafion 117	–	–	0.89	150	120	0.37	23

a 75 μm poly(tetrafluoroethylene-co-hexafluropropylene) (FEP) and 50 μm poly(ethylene-alt-tetrafluoroethylene) (ETFE). Details of the synthesis of the membranes can be found elsewhere [6]. Properties of the grafted and sulfonated membranes are shown in Table 1. Commercial Nafion® 105 and 117 membranes were used as reference materials.

Prior to the measurements Nafion membranes were purified by boiling for about 60 min in a 5% H_2O_2 solution followed by rinsing and soaking in warm deionized water. The membranes were then boiled in 0.5 M sulfuric acid for about 60 min and again rinsed with deionized water. The radiation-grafted membranes were purified with sulfuric acid and cleaned with water as described above.

2.2. *Conductivity*

Conductivities were recorded by impedance spectroscopy using data gathered in the frequency range 5–85 kHz. Measurements were done with an Autolab PGSTAT 20 instrument (Eco Chemie B.V., The Netherlands) supplied with FRA 2.4 software connected to a two-electrode cell with 0.071 cm^2 platinum electrodes. Membrane resistance was determined by extrapolating the linear part and/or the semicircle of the Nyquist plot to the real axis of the complex impedance spectrum. The conductivity was calculated from the resistance using the electrode area and membrane thickness, the latter measured with a micrometer.

Prior to the measurement of the dependence of conductivity on temperature the membranes were equilibrated with water vapor in a sealed vessel for a minimum of 3 days. The conductivity cell was flushed with an inert nitrogen flow humidified at 10 °C above the cell temperature in order to keep the membrane at 100% relative humidity (RH) during the measurements. In addition extra water was retained in the bottom of the cell. The temperature was raised in 10 °C intervals and the conductivity was recorded after equilibration.

To investigate the effect of the RH on the conductivity membranes were allowed to equilibrate over a saturated salt solution in a sealed vessel for a minimum of 10 days. During the measurements the appropriate salt solution was retained in the bottom of the cell.

2.3. *Gas permeability and kinetic data*

The reactant gas permeabilities and the kinetics of the ORR were measured with an Autolab PGSTAT 20 instrument (Eco Chemie B.V.) supplied with GPES 4.6 software in a microelectrode cell. The working electrode was a 50 μm platinum wire sealed in a glass capillary while a platinum wire gauze served as a counter electrode. The dynamic hydrogen reference electrode consisted of two 300 μm platinum wires sealed in a glass tube and coated galvanostatically with platinum black. To ensure good mechanical contact the reference and the counter electrodes were pushed against the membrane with the assistance of springs while the membrane holder and working electrode positions were fixed.

During the measurements the microelectrode cell was positioned in a glass vessel with a tight lid and the temperature of the vessel was controlled with water circulation. Extra water was retained in the bottom of the cell to keep the membranes humid during the measurements and in addition the inflowing gas stream ($\sim$1 ml s^{-1}) was humidified at 25 °C above the cell temperature and was directed at the membrane.

Prior to measurements the membranes were allowed to equilibrate with the bathing gas for at least 16 h. Impurities were removed by scanning the working

electrode potential repeatedly from the hydrogen evolution to the oxygen evolution potential until there was no further improvement in the resolution. In each experiment the current was corrected for background current, which was determined from a blank experiment using a nitrogen atmosphere.

Gas permeability data were obtained chronoamperometrically by stepping the potential from the zero current region to the mass transfer controlled region of the ORR or the hydrogen oxidation reaction (HOR). The diffusion coefficient D and solubility c could be determined from the current transient $I(t)$ of the modified Cottrell equation when both linear and spherical diffusion contribute to the overall current:

$$I(t) = \frac{nF\pi^{1/2}r^2D^{1/2}c}{t^{1/2}} + nF\pi rDc \quad (1)$$

where r is the radius of the electrode and all the other symbols have their usual meanings. The rate of gas diffusion and the area of the microelectrode were taken into account in choosing the appropriate time window [7–10].

In the kinetic measurements of the ORR a slow potential sweep (0.5 mV s^{-1}) from the zero current region to the mass transfer limited region was recorded. Tafel slopes and exchange current densities were determined as usual from the mass transfer corrected data [2].

2.4. *Fuel cell measurements*

Measurements of the performance and long-term stability of the membranes were made in a 5 cm^2 fuel cell (GlobeTech, Inc., USA) under similar conditions to ensure that the measurements were directly comparable. The cell operated with pure hydrogen and oxygen with flow rates of 1 ml s^{-1} under atmospheric pressure and at a temperature of 60 °C. Hydrogen was humidified 10 °C above the cell temperature and oxygen at the cell temperature. Commercial gas diffusion electrodes (20% Pt/C, 0.35 mg cm^{-2} of Pt, E-TEK ELAT®) coated with a Nafion solution (0.5–0.8 mg cm^{-2}) were clamped together with a wet membrane in the cell with a standard torque of 5.5 N m^{-1}. Hotpressing was not used because the membranes were required for spectroscopic analysis after the fuel cell test. This procedure naturally causes poor performance due to higher internal resistances in the fuel cell.

3. Results and discussion

3.1. *Conductivity*

Conductivities and area resistances of the membranes at room temperature are shown in Table 2. The experimental membranes have conductivities comparable to those of the Nafion membranes. Nevertheless, the area resistances are distinctly lower for the radiation-grafted membranes than for Nafion 117, which is expected as Nafion 117 is thicker than the experimental membranes.

The comparison of conductivities of the three PVDF based membranes reveals a trend: PVDFc-g-PSSA, the thinnest membrane, has the lowest conductivity and PVDFa-g-PSSSA, the thickest one, has the highest. A similar trend has also been detected for ETFE and FEP based radiation-grafted membranes [11, 12]. However, the opposite is observed when comparing area resistances: the thinnest PVDF membrane appears to have the lowest area resistance. Again a similar behavior has been reported for FEP based membranes [12].

The comparison of PVDFa-g-PSSA with the two PVDF-co-HFP based membranes is also interesting as these membranes have similar thicknesses but different water uptakes (Table 1) due to structural differences. The specific conductivities of these membranes appear to increase with increasing HFP content, decreasing crystallinity and increasing water uptake. However, whilst the addition of 6% HFP to PVDF matrix does not appear to affect the area resistance when 15% HFP is added it is lowered considerably.

FEP-g-PSSA has similar conductivity and area resistance to PVDF-co-HFP(15%)-g-PSSA, as expected on the basis of a similar water uptake in terms of water molecules per sulfonic acid group and thickness. In contrast, the conductivity of ETFE-g-PSSA is lower than expected. Although it has a significantly higher water uptake than PVDFb-g-PSSA and a similar thickness, the conductivities are comparable.

The variations in the conductivities of membranes based on PVDF and the difference in the conductivities

Table 2. Conductivities and area resistances of the membranes at room temperature and 100% RH and open circuit voltages at 60 °C

Membrane	Conductivity (mS cm^{-1})	Area resistance (mΩ cm^2)	OCP (V)
PVDFa-g-PSSA	50	240	0.950
PVDFb-g-PSSA	48	145	0.925
PVDFc-g-PSSA	16	130	0.780
PVDF-co-HFP(6%)-g-PSSA	63	250	0.935
PVDF-co-HFP(15%)-g-PSSA	110	100	0.880
FEP-g-PSSA	108	130	0.870
ETFE-g-PSSA	43	250	0.870
Nafion 117	51	390	–
Nafion 105	56	220	0.945

of ETFE-g-PSSA and PVDFb-g-PSSA may be due to dissimilar distribution of PSSA sidechains. The three PVDF films were obtained from different manufacturers and may have been processed differently and in addition the processing effect on films can vary with the thickness. The properties of the initial PVDFb and ETFE matrices differ due to inherent differences between these materials and to possible variations in the film processing. These differences may affect the grafting reaction and the distribution of the grafts, which affects the conductivity. The sidechain distribution is possibly more uneven in ETFE-g-PSSA than in the rest of the experimental membranes. Investigations of the poly(styrene sulfonic acid) distribution in the radiation-grafted membranes are in progress. Overall it appears that both a low crystallinity, accompanied by high water uptake, and a reduced thickness result in a low area resistance, which is advantageous for the fuel cell application due to reduced ohmic losses in the membrane.

The membrane conductivity decreases drastically with RH (Figure 1) as has been observed earlier both for Nafion 117 [13] and radiation-grafted membranes [14]. At 100% RH membranes with high water uptakes have high conductivities. As the RH decreases the water content of the membrane decreases parallel to the conductivity. This decrease is rapid until 84% RH is reached where all of the membranes have a similar water uptake of six to seven water molecules per sulfonic acid group. However, the experimental membranes have conductivities approximately of 5 mS cm^{-1} whereas the conductivities of the Nafion membranes are slightly higher, about 20 mS cm^{-1}. When the RH is below 80% changes in both conductivity and water uptake become smaller and no major differences between the membrane properties can be observed. The conductivity of a radiation-grafted membrane depends mainly on the number of sulfonic acid groups, their distribution and the membrane water content. An increase in the number of water molecules per sulfonic acid group is known to increase the proton conductivity due to a change in the proton transfer mechanism, to a mechanism similar to that found in bulk water [13, 15, 16] (N. Walsby et al., submitted). It appears that differences in the water uptake and conductivity above 84% RH are due to dissimilarities in the structure of the matrix material, such as flexibility. The experimental membranes considered here have similar PSSA contents and so it can be concluded that the differences in conductivity are due mainly to differences in water uptake and distribution of PSSA. Nafion membranes have broadly similar conductivities to those of the experimental membranes even though they have distinctly lower ion exchange capacities (IEC) (Table 1). Nafion membranes apparently have a more clustered structure than the radiation-grafted membranes (N. Walsby et al., submitted) and it appears that this in combination with a higher acidity is more favorable for proton transport. The state of the water in the membranes is further discussed elsewhere (N. Walsby et al., submitted).

The conductivities of the membranes increase approximately obeying an Arrhenius law in the temperature range 20–70 °C (Figure 2). Temperature affects the conductivities of all the membranes similarly excluding PVDFc-g-PSSA, for which the conductivity increases significantly with temperature. Consequently, at 60 °C all the membranes have conductivities sufficient for fuel cell applications. An unusual behavior is also detected in the change in the thickness of the PVDFc-g-PSSA membrane with increasing temperature. The thin PVDFc-g-PSSA expanded by 150% whilst for the rest of the membranes, the thickness increased by no more than 10% when the temperature increased from 20 to 70 °C. Changes in the conductivity as a function of temperature in Nafion 117 were attributed to changes in membrane morphology and water uptake [17], similar phenomena may occur in the radiation-grafted membranes. The exceptional changes in the thickness and conductivity of PVDFc-g-PSSA as a function of temperature might be due to changes in the membrane morphology.

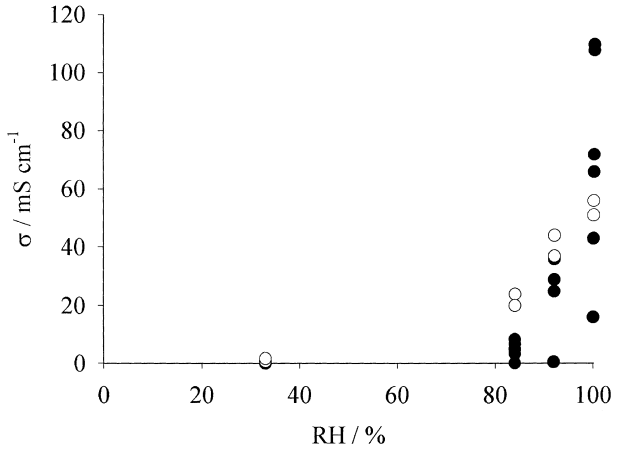

Fig. 1. Conductivities of (●) the radiation-grafted membranes and (○) Nafions at room temperature as a function of RH.

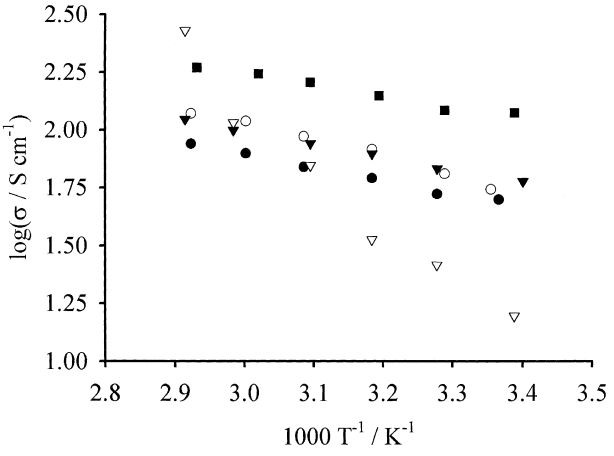

Fig. 2. Conductivity as a function of temperature (100% RH). (●) PVDFa-g-PSSA, (▽) PVDFc-g-PSSA, (▼) PVDF-co-HFP(6%)-g-PSSA, (■) PVDF-co-HFP(15%)-g-PSSA and (◯) Nafion 105.

Table 3. Oxygen permeabilities of the membranes at 20 °C

Membrane	$10^6\ D_{O_2}$ ($cm^2\ s^{-1}$)	$10^6\ c_{O_2}$ ($mol\ cm^{-3}$)	$10^{12}\ D_{O_2}c_{O_2}$ ($mol\ cm^{-1}\ s^{-1}$)	$10^9\ D_{O_2}c_{O_2}\ l^{-1}$ ($mol\ cm^{-2}\ s^{-1}$)
PVDFa	6.2	3.2	20	1.7
PVDFb	6.1	2.8	17	2.4
PVDF-co-HFP(6%)	6.3	2.0	12	1.1
PVDF-co-HFP(15%)	8.5	3.8	33	2.7
FEP	8.9	1.3	12	1.3
ETFE	6.4	1.9	12	2.1
Nafion 105	8.0	6.1	49	4.1
Nafion 117	1.1	9.3	10	0.50

3.2. *Gas permeability and kinetic data*

Oxygen diffusion coefficients, solubilities, permeabilities and fluxes for the membranes are presented in Table 3 excluding data for the PVDFc-g-PSSA membrane, which is so thin that Equation (1) could not be applied. At short times (<0.25 s) surface processes on the platinum electrode – especially in the case of hydrogen – caused the inverse square root of time dependence of the current to deviate substantially from linearity for all of the membranes.

The Nafion 117 oxygen diffusion coefficient (D_{O_2}) and solubility (c_{O_2}) are well in agreement with earlier results under similar experimental conditions, $0.24–2.8 \times 10^{-6}\ cm^2\ s^{-1}$ and $3.0–26 \times 10^{-6}\ mol\ cm^{-3}$ respectively [2, 18–20]. D_{O_2} appears to be of the same order of magnitude in Nafion 105 as in the radiation-grafted membranes whereas Nafion 117 has a slightly lower D_{O_2}. However, the c_{O_2} is distinctly lower in the experimental membranes than in the Nafions, which again may be due to differences in morphology and water uptake (N. Walsby et al., submitted). The structure of the hydrophilic domains is more homogenous in the radiation-grafted membranes than in Nafion. Altogether the experimental membranes appear to have oxygen fluxes between those of Nafion 117 and 105.

Although oxygen diffusion rates differ considerably in the initial matrix materials [21] they are of the same order of magnitude in the radiation-grafted membranes. Earlier investigations of this type of membranes have shown that both the oxygen diffusion and permeability increase with increasing water uptake and thus with DOG [2, 22, 23]. Water probably acts as a plasticizer in the membrane increasing the mobility of the chains and consequently facilitating gas transport. For Nafion it has been suggested that oxygen diffusion occurs in the hydrophobic intermediate region formed by the side chains [24] and for the Dow® Developmental membrane that it takes place in the aqueous phase [25]. In the radiation-grafted membranes diffusion apparently mainly occurs in the hydrophilic region. This explains both the similarity of the diffusion rates in the radiation-grafted membranes and the qualitative correspondence between the D_{O_2} and the water uptake.

For Nafion it has been shown that oxygen dissolves more readily in the hydrophobic than in the hydrophilic phase [26]. c_{O_2} in the experimental membranes is broadly similar and no clear trend can be detected. Differences in the oxygen solubilities reflect evidently both the inherent differences in the matrix materials and the processing effects.

The hydrogen solubility (c_{H_2}) and diffusion rate (D_{H_2}) for Nafion 117 (Table 4) are similar to literature values, $3.00–6.4 \times 10^{-6}\ mol\ cm^{-3}$ and $1.8–2.69 \times 10^{-6}\ cm^2\ s^{-1}$ respectively [18, 27]. In Nafion 117 hydrogen appears to diffuse significantly faster than oxygen but in the radiation-grafted membranes and in Nafion 105 both gases have broadly similar diffusion coefficients. Hydrogen solubilities appear to be somewhat higher than oxygen solubilities in the experimental membranes. This results in hydrogen permeabilities that are several times higher than oxygen permeabilities. Hydrogen fluxes appear to be slightly lower in Nafion 117, which is the thickest membrane, than in the radiation-grafted membranes or in Nafion 105. On the whole hydrogen solubilities and diffusion rates in the radiation-grafted membranes are more unequal than those of oxygen. No clear trend can be observed between membrane properties and hydrogen permeability. As a smaller molecule, hydrogen can probably permeate through both the

Table 4. Hydrogen permeabilities of the membranes at 20 °C

Membrane	$10^6\ D_{H_2}$ ($cm^2\ s^{-1}$)	$10^6\ c_{H_2}$ ($mol\ cm^{-3}$)	$10^{12}\ D_{H_2}c_{H_2}$ ($mol\ cm^{-1}\ s^{-1}$)	$10^9\ D_{H_2}c_{H_2}\ l^{-1}$ ($mol\ cm^{-2}\ s^{-1}$)
PVDFa	9.2	5.0	46	4.6
PVDFb	5.6	8.6	48	6.9
PVDF-co-HFP(6%)	12	4.7	55	5.0
PVDF-co-HFP(15%)	5.7	9.1	52	4.3
FEP	11	8.5	97	11
ETFE	9.1	4.2	38	6.4
Nafion 105	11	2.2	76	6.3
Nafion 117	17	7.0	38	1.9

hydrophilic and the hydrophobic phases of the membrane. Therefore inherent differences in the membranes affect the transport of hydrogen more than that of oxygen. Earlier investigations on radiation-grafted membranes have shown that hydrogen permeation is independent of the DOG [27], which supports this conjecture. The overall differences in the reactant gas fluxes appear to be insignificant.

For all the membranes two distinct Tafel slope regions are recorded for the ORR. At high potentials (900–800 mV vs DHE) the slopes are between 60 and 70 mV dec^{-1} and the exchange current densities are of the order 10^{-10}–10^{-9} A cm^{-2} apart from the two membranes with the highest water uptakes: PVDF-co-HFP(15%)-g-PSSA and FEP-g-PSSA have Tafel slopes slightly above 70 mV dec^{-1} and exchange current densities of the order 10^{-8} A cm^{-2}. Tafel slopes of 120–130 mV dec^{-1} are detected for all the membranes at low potentials (800–600 mV vs DHE) and exchange current densities of 10^{-7}–10^{-6} A cm^{-2} are estimated. For Nafion 117, Tafel slopes of 54 and 113 mV dec^{-1} with exchange current densities of 1.2×10^{-9} and 4.9×10^{-7} A cm^{-2}, respectively, were measured. These results are in agreement with earlier measurements [2, 19]. This kind of behavior with two Tafel slopes is typical for oxygen reduction on platinum in acidic media [28].

It appears that the ORR at lower potentials is somewhat enhanced when membranes with the high water uptakes and oxygen diffusion coefficients (PVDF-co-HFP(15%)-g-PSSA and FEP-g-PSSA) are used. However, there is some uncertainty in these kinetic measurements owing to less good repeatability and difficulties in controlling the RH, which varied between 95 and 100% from one measurement to another. Because kinetic properties depend somewhat on the membrane water content [29] and membranes dry out relatively easily in a humid gas atmosphere these results should be considered as semiquantitative.

3.3. *Fuel cell tests*

The membranes with high water uptakes have slightly lower open circuit potentials (OCP) than those with lower water uptakes (Table 2). The membranes were equilibrated with liquid water before assembling the cell, however, water uptake from the gaseous phase is less than from the liquid phase which results in the membrane shrinking under fuel cell conditions. These dimensional changes are considerable for membranes with a high water uptake, which may result in a poor contact between the electrodes and the membrane. Hydration of membranes with higher water uptake might also be incomplete which has been shown to result in a retarded ORR [29]. Superior OCPs, for example 0.93 V for ETFE-g-PSSA, are obtained when the membrane is dried before cell assembly, however in this case the water management in the fuel cell is difficult. These problems might be overcome by the design and optimization of separate anode and cathode electrodes and gas diffusion backings. For the thin PVDFc-g-PSSA (35 μm) membrane a low OCP is obtained suggesting substantial gas crossover.

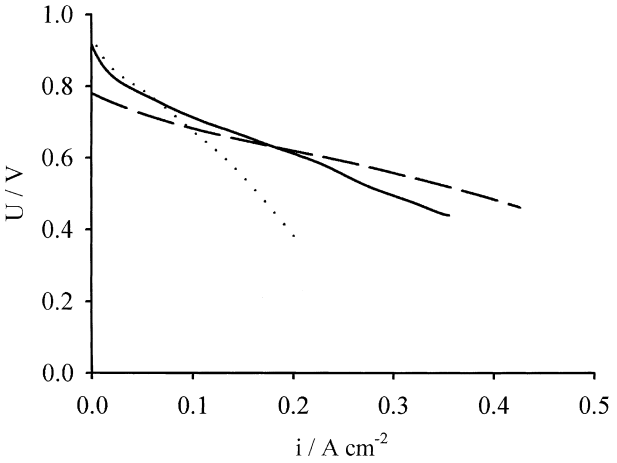

Fig. 3. Polarization curves for the PVDF based membranes at 60 °C and atmospheric pressure. (· · ·) PVDFa-g-PSSA, (—) PVDFb-g-PSSA and (– – –) PVDFc-g-PSSA.

The effect of the membrane area resistance on the polarization curves is clearly seen by comparing the three PVDF based membranes (Figure 3). Despite having the lowest OCP, the thinnest membrane, PVDFc-g-PSSA, has the best performance thanks to the lowest area resistance, while PVDFa-g-PSSA, with the highest area resistance, has the worst performance. Water management has been shown to be more straightforward in thinner membranes because problems caused by the uneven water distribution under fuel cell operation are alleviated, improving performance especially at high current densities [30]. The differences in the performance of the two PVDF-co-HFP and the PVDFa based membranes were in accordance with the differences in the area resistances. The FEP-g-PSSA and the ETFE-g-PSSA also showed similar performances to those of the two PVDF-co-HFP and the PVDFa based

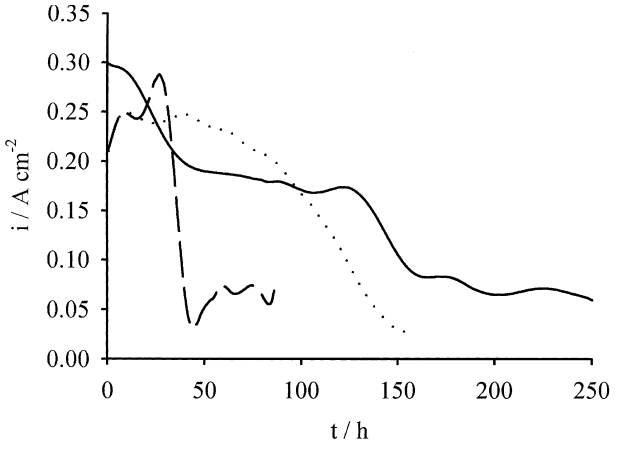

Fig. 4. Current densities of the PVDF based membranes vs time under 0.4 V constant load (60 °C, atmospheric pressure). (· · ·) PVDFa-g-PSSA, (—) PVDFb-g-PSSA and (– – –) PVDFc-g-PSSA.

membranes. Both of these former membranes had similar area resistances at 60 °C, due to changes in the conductivities and the thicknesses of the membranes as a function temperature, and OCPs similar to that of PVDF-co-HFP(15%)-g-PSSA. Under these fuel cell test conditions Nafion 105 had a slightly better performance than all but the two thinnest PVDF based membranes.

The durability of the radiation-grafted membranes was investigated by a constant voltage test (0.4 V) by following the changes in current density with time (Figure 4). The durabilities of these membranes were much lower than that of the Nafion membranes. Unfortunately all of the experimental membranes appeared to be mechanically unstable bar ETFE-g-PSSA. After the fuel cell test cracks were found near the interface between the electrode covered active area and the gasket sheltered inactive area. The formation is probably arising from the mechanical stress due to differences in membrane hydration in the inactive and active areas as suggested by Brack et al. [11]. Membranes with higher water uptake were observed to crack faster: PVDFc-g-PSSA and PVDF-co-HFP(15%)-g-PSSA failed mechanically in less than 50 h and FEP-g-PSSA in less than 80 h while in the rest of the membranes crack formation was observed between 150 and 200 h. These experimental membranes have similar mechanical properties at similar hydration levels [6] and thus the mechanical failure is apparently due to higher mechanical stress in membranes with higher water uptakes due to larger swelling.

As mentioned above, the long-term stability behavior of the ETFE-g-PSSA membrane differed from that of the other membranes. The current density of ETFE-g-PSSA decreased steadily over 150 h finally reaching the same level as the current densities of the other experimental membranes. However, no crack formation was observed but chemical degradation of the membrane was visible.

The gradual decreases in the current densities of the radiation-grafted membranes were probably due to chemical degradation of the membranes. The spectroscopic analyses for these fuel cell tested membranes are in progress and will be published later.

4. Conclusions

Conductivities and area resistances of the different radiation-grafted fluoropolymers are comparable to those of Nafion membranes at fuel cell operation temperatures and so in this aspect these membranes are suitable for fuel cell applications. Radiation-grafted membrane conductivity is apparently determined – at similar DOG – by the ability of the material to swell and absorb water. In general the conductivity increases with membrane thickness and water uptake.

Membranes intended for the fuel cells have to have a low reactant gas permeability to prevent a reduction in the cell efficiency owing to reactant gas mixing. In the experimental membranes the hydrogen flux appears to be several times higher than that of oxygen. No significant differences in either oxygen or hydrogen fluxes in the different radiation-grafted membranes are observed and they compare favorably with Nafion 105.

Above all membranes have to endure demanding fuel cell conditions. As expected, membranes with lower area resistances had better performances despite lower open circuit voltages. Nevertheless, these membranes with the best performances appeared to be less durable in the fuel cell. The reason for this is crack formation caused by a high mechanical stress due to uneven swelling and shrinking of the membrane at the border of the active and the inactive areas.

Overall, the reactant gas permeabilities appear not to essentially depend on the properties of the matrix material; instead these properties affect the conductivity and the durability under the fuel cell conditions. According to these results in a durable membrane the water uptake must be low even at the expense of the conductivity. An exception was the ETFE-g-PSSA membrane that did not crack under the fuel cell conditions but was chemically unstable. Apparently thin membranes (under 40 μm) are not appropriate for fuel cell application owing to poor mechanical properties and possible problems with high gas crossover.

The durability of these membranes may be improved either by crosslinking or lowering the DOG, which decrease the membrane water uptake. In addition the fuel cell operation conditions have to be optimized. Due to the advantages of the radiation-grafting method, especially the low cost of the matrix polymers and the preparation, the investigation of the radiation-grafted membranes will be continued.

Acknowledgements

The Academy of Finland and the graduate school Electrochemical Science and Technology of Polymers and Membranes including Biomembranes (ESPOM) are gratefully acknowledged for financial support.

References

1. G. Inzelt, M. Pineri, J.W. Schultze and M.A. Vorotyntsev, *Electrochim. Acta* **45** (2000) 2403.
2. T. Lehtinen, G. Sundholm, S. Holmberg, F. Sundholm, P. Björnbom and M. Bursell, *Electrochim. Acta* **43** (1998) 1881.
3. H.-P. Brack, H.G. Büchi, L. Bonorand and G.G. Scherer, *J. Mater. Chem.* **10** (2000) 1795.
4. M. Nasef, H. Saidi and M.A. Yarmo, *J. New Mat. Electrochem. Systems* **3** (2000) 309.
5. H. Wang and G.A. Capuano, *J. Electrochem. Soc.* **145** (1998) 781.
6. N. Walsby, F. Sundholm, T. Kallio and G. Sundholm, *J. Polym. Sci. Part A: Polym. Chem.* **39** (2001) 3008.
7. K. Aoki and J. Osteryoung, *J. Electroanal. Chem.* **122** (1981) 19.
8. K. Aoki and J. Osteryoung, *J. Electroanal. Chem.* **125** (1981) 315.
9. K. Aoki and J. Osteryoung, *J. Electroanal. Chem.* **160** (1984) 335.
10. C.P. Winlove, K.H. Parker and R.E. White, *J. Electrochem. Soc.* **170** (1984) 293.

11. H.-P. Brack, F.N. Büchi, J. Huslage and G.G. Scherer, *Proceedings of 194th ECS Meeting*, Boston 1998, p. 52.
12. H.-P. Brack and G.G. Scherer, *Macromol. Symp.* **126** (1997) 25.
13. T.A. Zawodzinski, Jr, M. Neeman, L.O. Sillerud and S. Gottesfield, *J. Phys. Chem.* **95** (1991) 6040.
14. S. Hietala, S.L. Maunu, F. Sundholm, T. Lehtinen and G. Sundholm, *J. Polym. Sci. Part B: Polym. Phys.* **37** (1999) 2893.
15. K.D. Kreuer, *Chem. Mater.* **8** (1996) 610.
16. K.D. Kreuer, T. Dippel and J. Maier, In *Proton Conducting Membrane Fuel Cells I*, S. Gottesfeld, G. Halpert and A. Landgrebe (eds), Proceedings/The Electrochemical Society 95-23, New Jersey 1995, p. 241.
17. P.C. Rieke and N.E. Vanderborgh, *J. Membr. Sci.* **32** (1987) 13.
18. K. Ota, Y. Inoue, N. Motohira and N. Kamiya, *J. New Mat. Electrochem. System* **3** (2000) 193.
19. A. Parthasarathy, C.R. Martin and S. Srinivasan, *J. Electrochem. Soc.* **138** (1991) 916.
20. A.T. Haug and R.E. White, *J. Electrochem. Soc.* **147** (2000) 980.
21. Polymer Handbook, J. Brandrup, E.H. Immergut and E.A. Grulke (eds), 4th edn (John Wiley & Sons, New York 1999, VI/547).
22. S. Hietala, E. Skou and F. Sundholm, *Polymer* **40** (1999) 5567.
23. C. Chuy, V.I. Basura, E. Simon, S. Holdcroft, J. Horsfall and K.V. Lovell, *J. Electrochem. Soc.* **147** (2000) 4453.
24. Z. Ogumi, T. Kuroe and Z. Takehara, *J. Electrochem. Soc.* **132** (1985) 2601.
25. Y. Tsou, M. Kimble and R.E. White, *J. Electrochem. Soc.* **139** (1992) 1913.
26. F.N. Büchi, M. Wakizoe and S. Srinivasan, *J. Electrochem. Soc.* **143** (1996) 927.
27. T. Lehtinen, G. Sundholm and F. Sundholm, *J. Appl. Electrochem.* **29** (1999) 677.
28. A. Damjanovic, D.B. Sepa and M.V. Vjonovic, *Electrochim. Acta* **24** (1979) 887.
29. F.A. Uribe, T.E. Springer and S. Gottesfeld, *J. Electrochem. Soc.* **139** (1992) 765.
30. T.E. Springer, T.A. Zawodzinski and S. Gottesfeld, *J. Electrochem. Soc.* **138** (1991) 2334.